Softness Effects on Manipulability and Grasp Stability

Tetsuyou Watanabe

***Abstract*— This paper presents a novel analysis for the effects of softness at the fingertip on the manipulability and stability of grasping. The stability for grasping can be regarded that how much magnitude of external wrench we can balance. We formulate manipulability and the set of generable object wrenches for grasping system, taking deformation of the fingertips into consideration, and show that the increase of the softness decreases the manipulability while it increases generable object wrench. The validity of our analysis is shown by numerical examples.**

I. Introduction

Recently, there is much attention on robots executing everyday manipulation in human environment [1]. Multi-fingered hand manipulation is necessary to execute such kind of tasks. If developing such robot hand systems, we should take the affinity to human into consideration. Therefore, grasping with deformable fingertips or contact areas have been researched [2]. They developed controller for grasping and manipulating the object with deformable fingertips. However, there are still many unclear issues about the effects of the softness around contact area (deformation of the fingertips). This paper focuses on and analyzes the effect of the softness at the contact area on manipulability and grasp stability: how much easily we can manipulate the object and how much magnitude of external wrench we can compensate.

Manipulability is a well-known concept to evaluate the performance of robotic manipulator [3]. For a single-arm manipulator, it is defined as the set of generable end-effector velocities in the task space when the set of generable joint velocities is given. When the given set of joint velocities is a unit ball, the set of end-effector velocities becomes an ellipsoid. The ellipsoid is called manipulability ellipsoid. The volume of the ellipsoid can be regarded as a quality measure to evaluate the performance in velocity domain. It is called manipulability measure. Based on the manipulability, many quality measures such as condition number are proposed [3]. This concept can be extended to the general constraining system such as robotic hands [4]–[10]. In a general constraining system, object velocity is evaluated instead of endeffector velocity. For a dual-arm system, Chiacchio et al. [4] discussed manipulability. Bicchi et al. [5] analyzed manipulability for general grasping system including whole arm manipulation system. After that, Bicchi et al. [6], Wen et al. [7], and Park et al. [8] analyzed manipulability for general constraining systems with underactuated joints. T. Watanabe [9], [10] presented a way for manipulability analysis taking joint torques required for grasping into consideration. However no-researchers concerned the softness effects on manipulability for grasping systems.

The magnitude of generable resultant object wrench has been regarded as a criterion index representing grasping stability since it corresponds to how much magnitude of external wrench we can compensate. By linearizing the frictional cone [11], the set of generable resultant object wrench can be expressed by a convex polyhedron. Then, the volume of the set can be calculated by, for example, qhull algorithm [12], and it can be a criterion index. The radius of the sphere inscribed the set can also be a criterion index since it represents the maximum magnitude of external wrench which can be balanced in any direction. These criterion indexes are embedded in GRASPIT [13] which is simulation software for grasp planning. Based on these kinds of criterion indexes, grasp planning problems such as investigations of grasping points and posture have been researched. On the other hand, if the contact area is deformable, the moment around normal direction can be applied. Such a contact is called soft-finger contact model, and corresponding frictional condition was researched [14], [15]. However, it is not clear how the change of the softness around contact area affects friction and the generable resultant object wrench.

Concerning these, this paper gives the following contributions.

Criterion index for manipulability including softness effect: We formulate kinematical relationship between fingertip, contact and object velocities, taking the softness effect (deformation of contact area) into consideration. Then, we construct the set of generable object velocities under the bound on the magnitude of fingertip velocities. From the derived set of generable object velocities, we present new criterion index for manipulability which can take the softness effect into consideration.

Criterion index for grasp stability including softness effect: We formulate frictional conditions based on the contact area associated with the deformation of fingertip, which can explicitly represent how the change of the softness affects friction. Linearizing the formulated frictional conditions, we construct the set of generable object wrenches, expressed by a convex polyhedron. From the set, we derive the new criterion index for grasp stability which can take the softness effect into consideration.

Softness effect on manipulability and grasp stability: Based on the derived criterion index, we analytically show the decrease of softness (increase of stiffness) causes the increase of manipulability. It will be also shown by numerical

This work was not supported by any organization

T. Watanabe are with College of Science and Engineering, Kanazawa University, Kanazawa, 920-1192, Japan and te-watanabe@ieee.org

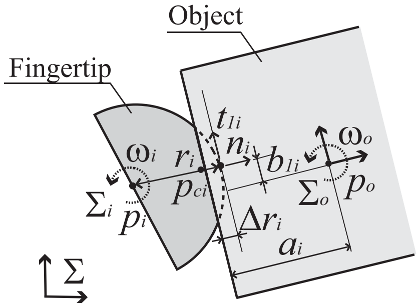

Fig. 1. Model for analysis

examples. We also show the decrease of softness (increase of stiffness) causes the decrease of grasp stability: we can balance larger external object wenches with softer fingertips.

The rest of this paper is organized as follows. First, we formulate the criterion indexes for manipulability and grasp stability. After that, we show the numerical examples to confirm the analysis.

II. Softness effects

A. Effect on manipulability

Here, we discuss manipulability [3] to understand how easily the hand can manipulate the object. Fig.1 shows the model of the fingertip and the object. This model is based on the models of Xydas et. al. [15] and Arimoto et. al. [16]. For the convenient, we discuss only fingertip motion, and assume that we can move the fingertip in arbitrary directions. Every fingertip has a shape of deformable hemisphere. The object has flat surface at the contact point and is rigid body. We consider to grasp the object with n fingertips. Let Σ_o and Σ_i be the coordinates located at the gravity center of the object and at the center of hemisphere of ith fingertip. Let be $\boldsymbol{p}_o$ and $\boldsymbol{p}_i$ are the positions of the origin of Σ_o and Σ_i, and $\boldsymbol{p}_{ci}$ be the position of the center of the contact surface between the ith fingertip and the object. $\boldsymbol{\omega}_o$ and $\boldsymbol{\omega}_i$ are angular velocities of Σ_o and Σ_i. $\boldsymbol{n}_i$ is unit contact normal directing inside of the object. $\boldsymbol{t}_{1i}$ and $\boldsymbol{t}_{2i}$ are unit contact tangential vectors. r_i is the hemisphere radius of the fingertip and Δr_i is the deformation amount by contact. Let f_{ni} be the component of contact force in normal direction $\boldsymbol{n}_i$. We assume the following relation at the steady state.

$$f_{ni} = k_i \Delta r_i^{\zeta} \tag{1}$$

where k_i and ζ are material and geometric parameters associated with softness. Note that if according to the models of Arimoto [16] and Inoue et. al. [17], $\zeta = 2$. If supposing grasping the object with certain constant contact forces, we can regard Δr_i as a parameter expressing skin softness. If Δr_i is large, it means the skin is soft and vice versa.

The relationship between $\boldsymbol{p}_{ci}$ and $\boldsymbol{p}_i$ is given by

$$\boldsymbol{p}_{ci} = \boldsymbol{p}_i + (r_i - \Delta r_i)\boldsymbol{n}_i \tag{2}$$

If differentiating this relationship with respect to time, we get

$$\dot{\boldsymbol{p}}_{ci} = \dot{\boldsymbol{p}}_i + (r_i - \Delta r_i)(\boldsymbol{\omega}_i \times \boldsymbol{n}_i) + \boldsymbol{v}_i - \Delta\dot{r}_i \boldsymbol{n}_i \tag{3}$$

where

$$\boldsymbol{v}_i = (r_i - \Delta r_i)(\dot{\boldsymbol{n}}_i - \boldsymbol{\omega}_i \times \boldsymbol{n}_i)$$

expresses the surface velocity on the ith fingertip.

On the other hand, the relationship between $\boldsymbol{p}_{ci}$ and $\boldsymbol{p}_o$ is given by

$$\boldsymbol{p}_{ci} = \boldsymbol{p}_o - a_i\boldsymbol{n}_i + b_{1i}\boldsymbol{t}_{1i} + b_{2i}\boldsymbol{t}_{2i} \tag{4}$$

where a_i , b_{1i} and b_{2i} denote the distances between Σ_o and $\boldsymbol{p}_{ci}$ along the directions of $\boldsymbol{n}_i$, $\boldsymbol{t}_{1i}$ and $\boldsymbol{t}_{2i}$, respectively. Note that a_i is constant since it represents the distance between Σ_o and the side of the object. If differentiating this relationship with respect to time, we get

$$\begin{aligned}\dot{\boldsymbol{p}}_{ci} = \dot{\boldsymbol{p}}_o &+ \boldsymbol{\omega}_o \times (-a_i\boldsymbol{n}_i + b_{1i}\boldsymbol{t}_{1i} + b_{2i}\boldsymbol{t}_{2i}) \\ &- \dot{a}_i\boldsymbol{n}_i + \dot{b}_{1i}\boldsymbol{t}_{1i} + \dot{b}_{2i}\boldsymbol{t}_{2i}\end{aligned} \tag{5}$$

From (3) and (5), the following equation is obtained.

$$\begin{aligned}&\dot{\boldsymbol{p}}_i + (r_i - \Delta r_i)(\boldsymbol{\omega}_i \times \boldsymbol{n}_i) - \Delta\dot{r}_i\boldsymbol{n}_i \\ &\quad = \dot{\boldsymbol{p}}_o + \boldsymbol{\omega}_o \times (-a_i\boldsymbol{n}_i + b_{1i}\boldsymbol{t}_{1i} + b_{2i}\boldsymbol{t}_{2i})\end{aligned} \tag{6}$$

Here we used the following relationships:

$$\dot{a}_i = 0,\ \boldsymbol{v}_i = \dot{b}_{1i}\boldsymbol{t}_{1i} + \dot{b}_{2i}\boldsymbol{t}_{2i}$$

which expresses there is no slippage between the fingertip and the object (the surface velocity on the fingertip is equal to the one on the object surface) and is non-holonomic constraint.

On the other hand, if fingertip is soft, then the angular velocity around the contact normal direction can be applied to the object.

$$\boldsymbol{n}_i^T\boldsymbol{\omega}_i = \boldsymbol{n}_i^T\boldsymbol{\omega}_o. \tag{7}$$

From (6) and (7), we get

$$\boldsymbol{G}_{fi}^T \begin{bmatrix} \dot{\boldsymbol{p}}_i \\ \boldsymbol{\omega}_i \end{bmatrix} = \boldsymbol{n}_i\Delta\dot{r}_i + \boldsymbol{G}_{oi}^T \begin{bmatrix} \dot{\boldsymbol{p}}_o \\ \boldsymbol{\omega}_o \end{bmatrix} \tag{8}$$

where

$$\begin{aligned}\boldsymbol{G}_{fi}^T &= \boldsymbol{G}_{fri}^T + \Delta r_i \boldsymbol{G}_{fdi}^T, \\ \boldsymbol{G}_{fri}^T &= \begin{bmatrix} \boldsymbol{I}_{3\times3} & -r_i[\boldsymbol{n}_i\times] \\ \boldsymbol{O}_{1\times3} & \boldsymbol{n}_i^T \end{bmatrix}, \\ \boldsymbol{G}_{fdi}^T &= \begin{bmatrix} \boldsymbol{O}_{3\times3} & [\boldsymbol{n}_i\times] \\ \boldsymbol{O}_{1\times3} & \boldsymbol{O}_{1\times3} \end{bmatrix}, \\ \boldsymbol{G}_{oi}^T &= \begin{bmatrix} \boldsymbol{I}_3 & -[(-a_i\boldsymbol{n}_i + b_{1i}\boldsymbol{t}_{1i} + b_{2i}\boldsymbol{t}_{2i})\times] \\ \boldsymbol{O}_{1\times3} & \boldsymbol{n}_i^T \end{bmatrix}\end{aligned} \tag{9}$$

If aggregating (8) for all n contact points, we get

$$\boldsymbol{G}_f^T\dot{\boldsymbol{x}}_f = \boldsymbol{N}\Delta\dot{\boldsymbol{r}} + \boldsymbol{G}_o^T\dot{\boldsymbol{x}}_o := \dot{\tilde{\boldsymbol{p}}}_c \tag{10}$$

where

$$\dot{\boldsymbol{x}}_{fi} = \begin{bmatrix} \dot{\boldsymbol{p}}_i \\ \boldsymbol{\omega}_i \end{bmatrix},\ \dot{\boldsymbol{x}}_f = \begin{bmatrix} \dot{\boldsymbol{x}}_{f1} \\ \dot{\boldsymbol{x}}_{f2} \\ \vdots \\ \dot{\boldsymbol{x}}_{fn} \end{bmatrix},\ \dot{\boldsymbol{x}}_o = \begin{bmatrix} \dot{\boldsymbol{p}}_o \\ \boldsymbol{\omega}_o \end{bmatrix}$$

$$\boldsymbol{G}_f^T = \mathrm{diag}[\boldsymbol{G}_{fi}^T],\ \boldsymbol{N} = \mathrm{diag}[\boldsymbol{n}_i],\ \boldsymbol{G}_o^T = \begin{bmatrix} \boldsymbol{G}_{o1}^T \\ \boldsymbol{G}_{o2}^T \\ \vdots \\ \boldsymbol{G}_{on}^T \end{bmatrix}$$

where diag expresses a block diagonal matrix.

Then, we consider manipulability; how much magnitude of the object velocity ($\dot{\boldsymbol{x}}_o$) we can generate with the fingertip velocity ($\dot{\boldsymbol{x}}_f$) whose magnitude is bounded. We consider the generable object velocity under

$$\dot{\boldsymbol{x}}_f^T \boldsymbol{W}_f \dot{\boldsymbol{x}}_f \le 1 \tag{11}$$

where $\boldsymbol{W}_f$ denotes the weight matrix which is a positive definite symmetric matrix.

$\boldsymbol{G}_f^T$ is a full row rank matrix. Then, from (10), we get

$$\dot{\boldsymbol{x}}_f = (\boldsymbol{G}_f^T)^+_{(wf)} \dot{\tilde{\boldsymbol{p}}}_c + (\boldsymbol{I} - (\boldsymbol{G}_f^T)^+_{(wf)} \boldsymbol{G}_f^T)\boldsymbol{k}_f \tag{12}$$

where $(\boldsymbol{G}_f^T)^+_{(wf)} = \boldsymbol{W}_f^{-1}\boldsymbol{G}_f(\boldsymbol{G}_f^T\boldsymbol{W}_f^{-1}\boldsymbol{G}_f)^{-1}$ denotes the weighted psedo-inverse matrix of $\boldsymbol{G}_f$ and $\boldsymbol{k}_f$ denotes an arbitrary vector. Similarly to the analyses of Yoshikawa [3] and Bicchi [18], we condier the generable $\dot{\tilde{\boldsymbol{p}}}_c$ with miminum cost. Then we get the following relationship:

$$\begin{aligned} 1 &\ge \dot{\boldsymbol{x}}_f^T \boldsymbol{W}_f \dot{\boldsymbol{x}}_f \\ &= \dot{\tilde{\boldsymbol{p}}}_c^T (\boldsymbol{G}_f^T \boldsymbol{W}_f^{-1} \boldsymbol{G}_f)^{-1} \dot{\tilde{\boldsymbol{p}}}_c + \boldsymbol{k}_f^T (\boldsymbol{I} - (\boldsymbol{G}_f^T)^+_{(wf)} \boldsymbol{G}_f^T)^2 \boldsymbol{k}_f \\ &\ge \dot{\tilde{\boldsymbol{p}}}_c^T (\boldsymbol{G}_f^T \boldsymbol{W}_f^{-1} \boldsymbol{G}_f)^{-1} \dot{\tilde{\boldsymbol{p}}}_c. \end{aligned} \tag{13}$$

Here, we consider $\boldsymbol{N}\Delta\dot{\boldsymbol{r}} + \boldsymbol{G}_o^T \dot{\boldsymbol{x}}_o = \dot{\tilde{\boldsymbol{p}}}_c$ shown in (10). This relationship includes $\Delta\dot{\boldsymbol{r}}$, but does not include $\Delta\boldsymbol{r}$. Hence, if concerning the effect of $\Delta\boldsymbol{r}$ (softness) on the generable object velocity $\dot{\boldsymbol{x}}_o$, we only have to consider $\boldsymbol{G}_f^T \boldsymbol{W}_f^{-1} \boldsymbol{G}_f$. What (the norm of) $\boldsymbol{G}_f^T \boldsymbol{W}_f^{-1} \boldsymbol{G}_f$ is large means that we can generate large object velocity and vice versa. Then, we focus on $\boldsymbol{G}_f^T \boldsymbol{W}_f^{-1} \boldsymbol{G}_f$. For the convenient, we assume

$$\boldsymbol{G}_f^T \boldsymbol{W}_f^{-1} \boldsymbol{G}_f = \mathrm{diag}[\boldsymbol{G}_{fi}^T \boldsymbol{W}_{fi}^{-1} \boldsymbol{G}_{fi}]$$

which means $\boldsymbol{W}_f = \mathrm{diag}[\boldsymbol{W}_{fi}]$ can be held. From (9), we get

$$\begin{aligned} \boldsymbol{G}_{fi}^T \boldsymbol{W}_{fi}^{-1} \boldsymbol{G}_{fi} = &\boldsymbol{G}_{fri}^T \boldsymbol{W}_{fi}^{-1} \boldsymbol{G}_{fri} \\ &+ \Delta r_i (\boldsymbol{G}_{fri}^T \boldsymbol{W}_{fi}^{-1} \boldsymbol{G}_{fdi} + \boldsymbol{G}_{fdi}^T \boldsymbol{W}_{fi}^{-1} \boldsymbol{G}_{fri}) \\ &+ \Delta r_i^2 \boldsymbol{G}_{fdi}^T \boldsymbol{W}_{fi}^{-1} \boldsymbol{G}_{fdi} \end{aligned}$$

Here, we define the following two matrices, respectively, expressing the term which does not include Δr_i and the term including Δr_i.

$$\begin{aligned} \boldsymbol{G}_{fi}^T \boldsymbol{W}_{fi}^{-1} \boldsymbol{G}_{fi} &= \boldsymbol{G}_{1fi} + \boldsymbol{G}_{2fi} \\ \boldsymbol{G}_{1fi} &= \boldsymbol{G}_{fri}^T \boldsymbol{W}_{fi}^{-1} \boldsymbol{G}_{fri} \\ \boldsymbol{G}_{2fi} &= \Delta \boldsymbol{r}_i (\boldsymbol{G}_{fri}^T \boldsymbol{W}_{fi}^{-1} \boldsymbol{G}_{fdi} + \boldsymbol{G}_{fdi}^T \boldsymbol{W}_{fi}^{-1} \boldsymbol{G}_{fri}) \\ &\quad + \Delta \boldsymbol{r}_i^2 \boldsymbol{G}_{fdi}^T \boldsymbol{W}_{fi}^{-1} \boldsymbol{G}_{fdi} \end{aligned} \tag{14}$$

Here, we suppose that

$$\boldsymbol{W}_{fi} = \begin{bmatrix} \boldsymbol{W}_{fi_{11}} & \boldsymbol{O}_{3\times3} \\ \boldsymbol{O}_{3\times3} & w_{fi_{22}} \boldsymbol{I}_{3\times3} \end{bmatrix},\ \boldsymbol{W}_{fi_{11}} \in \mathcal{R}^{3\times3}. \tag{15}$$

Then, from (9), $\boldsymbol{G}_{2fi}$ can be rewritten by

$$\boldsymbol{G}_{2fi} = \begin{bmatrix} \frac{(\Delta r_i^2 - 2r_i\Delta r_i)}{w_{fi_{22}}}[\boldsymbol{n}_i\times][\boldsymbol{n}_i\times]^T & \boldsymbol{O}_{1\times3} \\ \boldsymbol{O}_{3\times1} & 0 \end{bmatrix} \preceq \boldsymbol{O}, \tag{16}$$

since $\Delta r_i \le r_i$. Here $\boldsymbol{O} \preceq \boldsymbol{A}$ means $\boldsymbol{A}$ is positive semi-deninite. From this relationship and (14), we can get the following relationship

$$\boldsymbol{G}_{fi}^T \boldsymbol{W}_{fi}^{-1} \boldsymbol{G}_{fi} = \boldsymbol{G}_{1fi} + \boldsymbol{G}_{2fi} \preceq \boldsymbol{G}_{1fi}. \tag{17}$$

From (16), it can be seen that (the norm of) $\boldsymbol{G}_{2fi}$ decreases with the increase of Δr_i, which indicates that (the norm of) $\boldsymbol{G}_f^T \boldsymbol{W}_f^{-1} \boldsymbol{G}_f$ decreases with the increase of Δr_i. Therefore, we can say that generable object velocity decreases with the increase of Δr_i. The magnitude of Δr_i depends on the contact force and stiffness at the contact area, as it can be seen from (1). If comparing two grasps where the magnitude of contact forces are the same but stiffness at the contact area is different, the generable object velocity for larger stiffness is larger than that for smaller stiffness.

On the other hand, from (17), it can be seen that generable object velocity when the deformation at the contact area causes is smaller than that when the deformation at the contact area can be neglected (fingertip is rigid).

Summarizing, softness (stiffness) affects manipulability, namely generable object velocity decreases with the increase of softness (decrease of stiffness).

Now, from(10) and (13), we have

$$\begin{aligned} 1 &\ge \dot{\boldsymbol{x}}_f^T \boldsymbol{W}_f \dot{\boldsymbol{x}}_f \\ &\ge (\boldsymbol{N}\Delta\dot{\boldsymbol{r}} + \boldsymbol{G}_o^T \dot{\boldsymbol{x}}_o)^T (\boldsymbol{G}_f^T \boldsymbol{W}_f^{-1} \boldsymbol{G}_f)^{-1} (\boldsymbol{N}\Delta\dot{\boldsymbol{r}} + \boldsymbol{G}_o^T \dot{\boldsymbol{x}}_o). \end{aligned} \tag{18}$$

This set can be regarded as an ellipsoid in $[\Delta\dot{\boldsymbol{r}}^T\ \dot{\boldsymbol{x}}_o^T]^T$ space. Here, we will consider to map this ellipsoid onto $\dot{\boldsymbol{x}}_o$ space. For this purpose, we consider the completing square with respect to $\Delta\dot{\boldsymbol{r}}$:

$$(\Delta\dot{\boldsymbol{r}} - \boldsymbol{A}_2\dot{\boldsymbol{x}}_o)^T \boldsymbol{A}_1 (\Delta\dot{\boldsymbol{r}} - \boldsymbol{A}_2\dot{\boldsymbol{x}}_o) + \dot{\boldsymbol{x}}_o^T \boldsymbol{A}_3 \dot{\boldsymbol{x}}_o \le 1. \tag{19}$$

where $\boldsymbol{A}_1$, $\boldsymbol{A}_2$ and $\boldsymbol{A}_3$ are the matrices derived by the completing square. From this formulation, it can be seen that the ellipsoid (18) is divided equally in $\Delta\dot{\boldsymbol{r}}$ direction by $\Delta\dot{\boldsymbol{r}} = \boldsymbol{A}_2\dot{\boldsymbol{x}}_o$(see Fig.2). If substituting $\Delta\dot{\boldsymbol{r}} = \boldsymbol{A}_2\dot{\boldsymbol{x}}_o$ into the ellipsoid (18), we get

$$\{\Delta\dot{\boldsymbol{r}} = \boldsymbol{A}_2\dot{\boldsymbol{x}}_o, \quad \dot{\boldsymbol{x}}_o^T \boldsymbol{A}_3 \dot{\boldsymbol{x}}_o \le 1\}$$

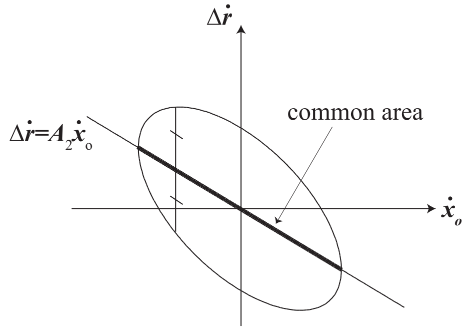

Fig. 2. Mapping of the ellipsoid onto $\dot{\boldsymbol{x}}_o$ space

which is common area of the ellipsoid (18) and $\Delta\dot{\boldsymbol{r}} = \boldsymbol{A}_2\dot{\boldsymbol{x}}_o$. In this set, $\dot{\boldsymbol{x}}_o^T\boldsymbol{A}_3\dot{\boldsymbol{x}}_o \leq 1$ expresses the feasible area/range of $\dot{\boldsymbol{x}}_o$ in the common area. This set is equivalent to the ellipsoid mapped onto $\dot{\boldsymbol{x}}_o$ space.

Comparing the coefficients of (18) and (19), we have

$$\boldsymbol{A}_1 = \boldsymbol{N}^T(\boldsymbol{G}_f^T\boldsymbol{W}_f^{-1}\boldsymbol{G}_f)^{-1}\boldsymbol{N}.$$

$\boldsymbol{A}_1$ is regular since $\boldsymbol{N}$ has full column rank. Then, $\boldsymbol{A}_2$ and $\boldsymbol{A}_3$ can be written by

$$\begin{aligned}\boldsymbol{A}_2 &= -\boldsymbol{A}_1^{-1}\boldsymbol{N}^T(\boldsymbol{G}_f^T\boldsymbol{W}_f^{-1}\boldsymbol{G}_f)^{-1}\boldsymbol{G}_o^T\\ &= \boldsymbol{N}^+_{((\boldsymbol{G}_f^T\boldsymbol{W}_f^{-1}\boldsymbol{G}_f)^{-1})}\boldsymbol{G}_o^T.\\ \boldsymbol{A}_3 &= \boldsymbol{G}_o(\boldsymbol{I} - \boldsymbol{N}\boldsymbol{N}^+_{((\boldsymbol{G}_f^T\boldsymbol{W}_f^{-1}\boldsymbol{G}_f)^{-1})})^T\\ &\quad (\boldsymbol{G}_f^T\boldsymbol{W}_f^{-1}\boldsymbol{G}_f)^{-1}(\boldsymbol{I} - \boldsymbol{N}\boldsymbol{N}^+_{((\boldsymbol{G}_f^T\boldsymbol{W}_f^{-1}\boldsymbol{G}_f)^{-1})})\boldsymbol{G}_o^T\end{aligned}$$

Now, we express the object velocity which we would like to evaluate, with weighted matrix $\boldsymbol{W}_o$:

$$\dot{\tilde{\boldsymbol{x}}}_o = \boldsymbol{W}_o\dot{\boldsymbol{x}}$$

Using this relationship, the generable object velocity can be expressed by the following ellipsoid:

$$\dot{\tilde{\boldsymbol{x}}}_o^T\boldsymbol{M}\dot{\tilde{\boldsymbol{x}}}_o \leq 1. \quad (20)$$
$$\boldsymbol{M} = \boldsymbol{W}_o^{-T}\boldsymbol{A}_3\boldsymbol{W}_o^{-1}$$

From this, we will define the following criterion index:

$$\mathcal{I}_m = \frac{1}{\sqrt{\lambda_{\max}(\boldsymbol{M})}}, \quad (21)$$

where $\lambda_{\max}(\boldsymbol{M})$ denotes the maximum eigenvalue of $\boldsymbol{M}$. This index expresses the maximum object velocity which is generable in any direction.

Remark that $\boldsymbol{M}$ includes $\boldsymbol{G}_{fi}$ given in (9), and $\boldsymbol{G}_{fi}$ includes Δr_i (see (1)). Then, we need to give not only fingertip configuration but also grasping force to determine $\boldsymbol{M}$.

B. Effect on stability/friction

We suppose that grasp stability means that we can balance large external wrench. Here, we analyze the effect of softness on how much magnitude of resultant wrench can be applied to the object. For the purpose, we focus on friction. There are some hypotheses for principle of friction, but normally, if two surfaces contacts each other, the total resistance force for tangential motion can be expressed by [19]

$$F_{tan} = A_{contact}\tau_{shearing} \quad (22)$$

where F_{tan} is the total resistance force, $A_{contact}$ is the true area of contact (The two surfaces actually touch at a discrete number of contact spots, and $A_{contact}$ corresponds to the sum of the all areas) and $\tau_{shearing}$ is the resistance force per unit area. If according to the model given by Persson [20]–[22], the real contact area corresponds to the apparent contact area if the contact surface is enough smooth and contact pressure is enough high. In other cases (which is usual), the real contact area is proportional to the load f_n (contact normal force):

$$A_{contact} = \frac{Q(1-\nu^2)f_n}{E} \quad (23)$$

where Q is the coefficient related with contact surface roughness, ν and E are Poisson's ratio and elastic modulus where $\frac{(1-\nu^2)}{E} = \frac{(1-\nu_1^2)}{E_1} + \frac{(1-\nu_2^2)}{E_2}$ (the subscript 1 and 2 corresponds to the two materials constructing the contact surface) In this case, maximum static frictional force is given by

$$F_{tan} = \mu_{soft}f_n, \quad \mu_{soft} = \frac{Q(1-\nu^2)\tau_{shearing}}{E} \quad (24)$$

μ_{soft} can be regarded as maximum static frictional coefficient. From this equation, we can see the relationship between frictional coefficient and elastic modulus, which was not considered in conventional analyses of grasping. If comparing the two fingertips whose softness (E) is different but whose $\tau_{shearing}$ is the same (for example, because the surface is made of the same material), μ_{soft} for the softer fingertip is larger than the other one, and then applicable frictional forces are also larger. This might be one of the reasons why grasping with softer fingertip can achieve more stable grasping.

In general, if the fingertip is deformable, it is called soft-finger contact. In this model, not only frictional forces but also contact moment around normal direction can be applied to the object. This paper also considers the contact moment. Similarly to the methodology of Xydas et. al. [15], we derive local frictional forces in tangential direction at local infinitesimal area of the contact area (from the contact pressure on that area), and then derive frictional forces and contact moment at the contact area by integrating the local frictional forces with respect to the whole contact area. By deriving the local frictional forces according to (24), the frictional condition can be represented by

$$\mathcal{F}_i = \{\boldsymbol{f}_i, m_i | \frac{|\boldsymbol{f}_{ti}|^2}{(\mu_i f_{ni})^2} + \frac{|m_i|^2}{(\alpha_i a_{ci}\mu_i f_{ni})^2} \leq 1, f_{ni} \geq 0\}, \quad (25)$$
$$f_{ni} = \boldsymbol{n}_i^T\boldsymbol{f}_i,\ \boldsymbol{f}_{ti} = \boldsymbol{T}_i\boldsymbol{f}_i = \begin{bmatrix}\boldsymbol{t}_{1i}^T\\ \boldsymbol{t}_{2i}^T\end{bmatrix}\boldsymbol{f}_i.$$

where $\boldsymbol{f}_i$ is contact force vector, m_i is contact moment, μ_i is frictional coefficient corresponding to μ_{soft} in (24), $\boldsymbol{f}_{ti}$ is tangential force vector, a_{ci} is the radius of the contact area, and α_i is constant number.

Xydas et.al. [15] presented the relationship between radius of contact area a_{ci} and contact normal force f_{ni}

$$a_{ci} = \alpha_{ci} f_{ni}^{\gamma} \tag{26}$$

where $\alpha_{ci}^2 = 2r_i/k_i^{2\gamma}$ and $\zeta = 1/(2\gamma)$ $(0 \leq \gamma \leq 1/3)$. From (25) and (26), frictional condition can be rewritten by

$$\mathcal{F}_i = \{\boldsymbol{f}_i, m_i | \frac{|\boldsymbol{f}_{ti}|^2}{(\mu_i f_{ni})^2} + \frac{|m_i|^2}{(\mu_{mi} f_{ni}^{1+\gamma})^2} \leq 1, f_{ni} \geq 0\}, \tag{27}$$

$$\mu_{mi} = \alpha_i \alpha_{ci} \mu_i$$

μ_{mi} can be regarded as frictional coefficient for moment. This condition equals to conventional frictional condition for soft-finger contact, if assuming $\gamma = 0$ which corresponds to the case when the radius is proportional to contact normal force. Then it can be said that this condition is the extension of conventional frictional condition.

From (10) and the principle of virtual work, we have

$$\begin{bmatrix} \boldsymbol{w}_f \\ \boldsymbol{w}_o \end{bmatrix} = \begin{bmatrix} \boldsymbol{G}_f \\ \boldsymbol{G}_o \end{bmatrix} \boldsymbol{w}_c \tag{28}$$

where $\boldsymbol{w}_c = [\boldsymbol{w}_{c1}^T \ \boldsymbol{w}_{c2}^T \ \cdots]^T$, $\boldsymbol{w}_{ci} = [\boldsymbol{f}_i^T \ m_i]^T$, $\boldsymbol{w}_f$ denotes fingertip wrench corresponding to contact force $\boldsymbol{f}_i$ and contact moment m_i, $\boldsymbol{w}_o$ denotes resultant wrench applied to the object.

Now, supposing the upper bound of contact normal force is ξ_i, we represent the generable object wrench set as convex polyhedron. If tangential contact forces are zero, maximum magnitude of generable frictional moment around contact normal direction is given by

$$\mu_{mmi} f_{ni}^{1+\gamma}.$$

Fig. 3 shows the relationship between this maximum frictional moment and contact normal force. It can be seen from this figure that if contact normal force is very small, generable moment is almost zero, and as the contact normal force increases, the moment becomes to be generable. Then, we approximate this relationship by the two lines, as shown in Fig. 3. The dot line in Fig. 3 is the tangent line of the curve at the point where contact normal force is half of its maximum. Let ξ_{0i} be the contact normal force at the boundary (between the range where frictional moment can be generated and the range where it cannot). Note that ξ_{0i} is supposed to be small compared to ξ_i. Then, the generable maximum frictional moment can be represented by

$$\mu_{mmi}(f_{ni} - \xi_{0i})$$

where μ_{mmi} denotes the gradient of the approximated line. Based on this approximation, firstly, we consider the case when contact normal force f_{ni} is its maximum ξ_i. If contact normal force is fixed, the set of contact wrenches satisfying frictional condition can be represented by ellipsoid shown in

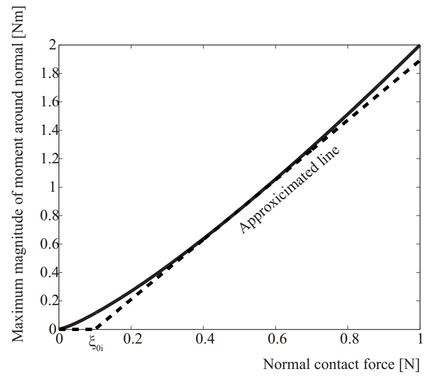

Fig. 3. Relation between maximum moment around contact normal and normal force (tangential force is zero and $\mu_{mi} = 2$, $\gamma = 0.25$)

Fig. 4. Extending the formulation of Yu and Wenhan [23], we approximate this ellipsoid by convex polyhedron.

$$\boldsymbol{w}_{ci} = \sum_{k=1}^{L}\sum_{\kappa=1}^{K-1} \lambda_{i_{k\kappa}} \boldsymbol{w}_{vi_{k\kappa}} + \lambda_{i_{10}} \boldsymbol{w}_{vi_{10}} + \lambda_{i_{1K}} \boldsymbol{w}_{vi_{1K}},$$
$$\sum_{k=1}^{L}\sum_{\kappa=1}^{K-1} \lambda_{i_{k\kappa}} + \lambda_{i_{10}} + \lambda_{i_{1K}} = 1, \quad \lambda_{i_{k\kappa}} \geq 0 \tag{29}$$
$$\boldsymbol{w}_{vi_{k\kappa}} = \xi_i \begin{bmatrix} \boldsymbol{n}_i \\ 0 \end{bmatrix} + \mu_i \xi_i \cos(\frac{2\pi k}{L}) \sin(\frac{\pi\kappa}{K}) \begin{bmatrix} \boldsymbol{t}_{1i} \\ 0 \end{bmatrix}$$
$$+ \mu_i \xi_i \sin(\frac{2\pi k}{L}) \sin(\frac{\pi\kappa}{K}) \begin{bmatrix} \boldsymbol{t}_{2i} \\ 0 \end{bmatrix}$$
$$+ \mu_{mmi}(\xi_i - \xi_{0i}) \cos(\frac{\pi\kappa}{K}) \begin{bmatrix} \boldsymbol{o}_{3\times 1} \\ 1 \end{bmatrix}$$

where K is number of the segments in moment direction and L is number of the segments in tangential direction. Note that $k = 1$ only when $\kappa = 0, K$, and $k = 1, 2, \cdots, L$ in the other cases. By reallocating the number, (29) is rewritten by

$$\boldsymbol{w}_{ci} = \sum_{k=1}^{\hat{l}} \lambda_{i_k} \boldsymbol{w}_{vi_k}, \quad \sum_{k=1}^{\hat{l}} \lambda_{i_k} = 1, \quad \lambda_{i_k} \geq 0$$
$$(k = 1, 2, \cdots, \hat{l} = L(K-1) + 2) \tag{30}$$

By the convex polyhedron whose vertexes are this $\boldsymbol{w}_{vi_k}$ and the point where $f_{ni} = \xi_{0i}$ and the other components are all zero (see Fig. 5), we approximate generable contact wrench set:

$$\boldsymbol{w}_{ci} = \sum_{k=1}^{l} \lambda_{i_k} \boldsymbol{w}_{vi_k}, \quad \sum_{k=1}^{l} \lambda_{i_k} = 1, \quad \lambda_{i_k} \geq 0$$
$$(k = 1, 2, \cdots, l = L(K-1) + 3), \tag{31}$$
$$\boldsymbol{w}_{vi_l} = \xi_{0i} \begin{bmatrix} \boldsymbol{n}_i \\ 0 \end{bmatrix}$$

Now we will construct grasp wrench space (the set of generable object wrenches) similarly to the way of Ferrari and Canny [24]. From (28), every $\boldsymbol{w}_{vi_k}$ in (31) is translated at the object frame

$$\boldsymbol{w}_{voi_k} = \boldsymbol{M}_{fo} \boldsymbol{G}_{oi} \boldsymbol{w}_{vi_k}$$

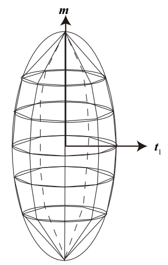

Fig. 4. Linearized frictional tangential forces and moment around the contact normal direction

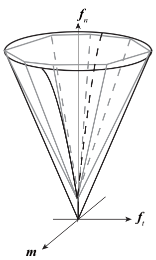

Fig. 5. Set of contact wrench satisfying frictional condition and approxi-cimated convex polyhedron (dashed line)

where $\boldsymbol{M}_{fo}$ is weight matrix. Then, bounding the sum magnitude of normal contact force, the grasp wrench space is given by

$$\mathcal{CH}(\bigcup_{i}^{n}(\boldsymbol{w}_{voi_1}, \boldsymbol{w}_{voi_2}, \cdots, \boldsymbol{w}_{voi_l})) \tag{32}$$

where $\mathcal{CH}$ denotes the convex hull, and the maximum summation of normalized normal contact forces by ξ_i is unit: $\sum_{i=1}^{n} |f_{ni}/\xi_i| \leq 1$. If bounding the magnitude of every normal contact force, the grasp wrench space is

$$\mathcal{CH}(\bigoplus_{i}^{n}(\boldsymbol{w}_{voi_1}, \boldsymbol{w}_{voi_2}, \cdots, \boldsymbol{w}_{voi_l})) \tag{33}$$

where $\bigoplus$ denotes the Minkowski sum, and the maximum normal contact forces is ξ_i for ith contact point.

We will have convex hulls of nl points in (32) while l^n points in (33). Therefore, from the viewpoint of computational effort, grasp wrench space given in (32) might be useful. In both cases, the grasp wrench space can be transformed into the following form:

$$\{\tilde{\boldsymbol{w}}_o \mid \boldsymbol{A}\tilde{\boldsymbol{w}}_o \leq \boldsymbol{b}\} \tag{34}$$

where $\boldsymbol{A}$ and $\boldsymbol{b}$ are the matrix and vector resulted from the transformation.

Let $\boldsymbol{A}=$ col$[\boldsymbol{a}_i^T]$ and $\boldsymbol{b}=$ col$[b_i]$. Generally the distance between the origin and a hyperplane $\boldsymbol{a}_i^T\boldsymbol{w}_o = b_i$ in the space of $\tilde{\boldsymbol{w}}_o$ is given by $b_i/|\boldsymbol{a}_i|$. Therefore, if force closure is satisfied, the maximum resultant object wrench which is generable in any direction can be obtained by

$$\mathcal{I}_f = \min_i b_i/|\boldsymbol{a}_i|. \tag{35}$$

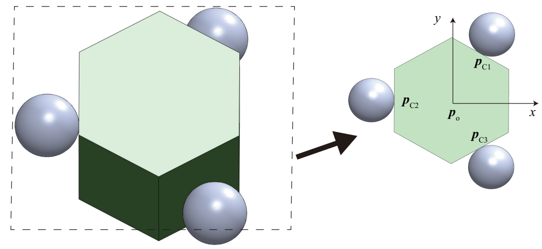

Fig. 6. Target system in numerical examples

TABLE I

PARAMETER VALUES FOR NUMERICAL EXAMPLES

Object base	regular hexagon (inradius: 0.025 (m))
Object height	0.1 (m)
r_i $(i = 1, 2, 3)$	0.01(m)
$\boldsymbol{W}_{fi}$	diag$[1\ 1\ 1\ r_i^2\ r_i^2\ r_i^2]$
$\boldsymbol{W}_f$	diag$[\boldsymbol{W}_{fi}]$
$\boldsymbol{W}_o$	diag[1 1 1 0.025 0.025 0.025]
$\boldsymbol{W}_{fo}$	diag[1 1 1 1/0.025 1/0.025 1/0.025]
$\boldsymbol{p}_o$	$[0\ 0\ 0]^T$(m)
$\boldsymbol{p}_{c1}$	$0.025[\cos(60°)\ \ \sin(60°)\ 0]^T$(m)
$\boldsymbol{p}_{c2}$	$0.025[\cos(120°)\ \ \sin(120°)\ 0]^T$(m)
$\boldsymbol{p}_{c3}$	$0.025[\cos(-60°)\ \ \sin(-60°)\ 0]^T$(m)
ξ_i	1 (N)
α_i	0.6
L	8
K	9
$Q(1-\nu^2)\tau_{shearing}$	$30000/\pi$ (N/m^2)
grasping force when calculating $\mathcal{I}_m$	$[-0.433\ \ -0.75\ \ 0\ \ 0.866\ \ 0\ \ 0\ \ -0.433\ \ 0.75\ \ 0]^T$

III. NUMERICAL EXAMPLES

In order to verify the validity of our approach, we show numerical examples. Fig.6 shows the target system where grasping the prism shaped object with 3 fingertips. Every fingertip is a sphere with the diameter of $r_i =$0.02 (m). The base is a regular hexagon whose inscribed circle is 0.025 (m) in radius, and the height of the object is 0.1 (m). We suppose that $k_i = \pi E$, based on (1) and the model of Inoue and Hirai [17]. We approximate fictional condition by convex polyhedron with 67 vertices where $L = 8$ and $K = 9$. We approximated the relationship between generable contact normal force and moment by the two lines, as shown in Fig. 3. The approximated line is the tangent line of the curve at the point where contact normal force is half of its maximum. The other setting parameters are listed at Table I.

Based on the setting, we calculated the criterion indexes $\mathcal{I}_m$ (in (21)) and $\mathcal{I}_f$ (in (35), derived using (32)). In order to investigate the influence of softness on manipulability index and grasp stability, we calculated $\mathcal{I}_m$ and $\mathcal{I}_f$ when changing stiffness parameter k_i (see (1)) from 10000 to 100000 (N/m^2) while ζ is 1.5, $1.5+1/6$, $1.5+1/3$, and 2. When calculating $\mathcal{I}_m$, the grasping forces (internal forces for grasping) is set as follows:

$$[-0.433\ \ -0.75\ \ 0\ \ 0.866\ \ 0\ \ 0\ \ -0.433\ \ 0.75\ \ 0]^T$$

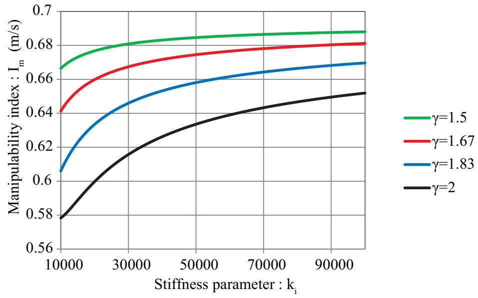

Fig. 7. Softness effect on manipulability: criterion index $\mathcal{I}_m$

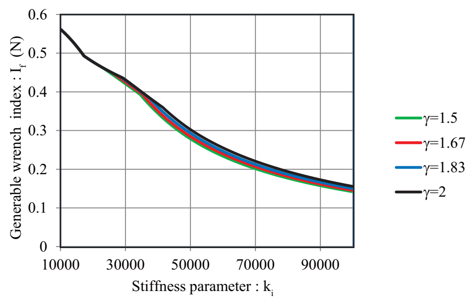

Fig. 8. Softness effect on generable object wrench: criterion index $\mathcal{I}_f$

The results are shown in Fig.7 and Fig.8. From Fig.7 and Fig.8, it can be seen that with the increase of stiffness parameter k_i, manipulability increases while generable object wrenches decrease. With the increase of γ, manipulability decreases while generable object wrenches increase. Both k_i and γ are the parameters related with softness. It is seemed that the effect of γ on manipulability is larger than that of k_i. On the other hand, the effect of k_i on generable object wrenches is larger than that of γ. Manipulability index depends on Δr_i, while generable object wrenches largely depend on k_i. They might be one of the reasons.

IV. Conclusion

In this paper, we analyzed the effects of softness at the fingertip on the manipulability and generable object wrenches. We formulated manipulability and the set of generable object wrench for grasping system, taking deformation of the fingertips into consideration. We showed that the increase of the softness decreases the manipulability while it increases generable object wrenches (stability from the view point of grasping). The validity of our approach was also shown by numerical examples. This analysis suggests that the softness of fingertip should change according to purpose of task, *if we can*. For example, when picking up (unknown) object on table, softer fingertip would be preferable. When assembling parts, harder fingertip would be preferable. In future, concerning this, we will develop a new system for fingertip, which can change stiffness of the fingertip.

References

[1] C. Kemp, A. Edsinger, and E. Torres-Jara, "Challenges for robot manipulation in human environments," *IEEE Robotics and Automation Magazine*, vol. 14, no. 1, pp. 20–29, 2007.

[2] K. Tahara, S. Arimoto, and M. Yoshida, "Dynamic object manipulation using a virtual frame by a triple soft-fingered robotic hand," *Proc. of the 2010 IEEE Int. Conf. Robot. Automat.*, pp. 4322–4327, 2010.

[3] T. Yoshikawa, *Foundations of Robotics*. MIT Press, Cambridge, 1990.

[4] P. Chiacchio, S. Chiaverini, L. Sciavicco, and B. Siciliano, "Global task space manipulability ellipsoids for multiple-arm systems," *IEEE Transactions on Robotics and Automation*, vol. 7, no. 5, pp. 678–685, 1991, correspondence.

[5] A. Bicchi, C. Melchiorri, and D. Balluchi, "On the mobility and manipulability of general multiple limb robots," *IEEE Transactions on Robotics and Automation*, vol. 11, no. 2, pp. 215–228, 1995.

[6] A. Bicchi and D. Prattichizzo, "Manipulability of cooperating robots with unactuated joints and closed-chain mechanisms," *IEEE Transactions on Robotics and Automation*, vol. 16, no. 4, pp. 336–345, 2000.

[7] J. T. Wen and L. S. Wilfinger, "Kinematic manipulability of general constrained rigid multibody systems," *IEEE Transactions on Robotics and Automation*, vol. 15, no. 3, pp. 558–567, 1999.

[8] F. C. Park and J. W. Kim, "Manipulability and singularity analysis of multiple robot systems: A geometric approach," *Proc. of IEEE International Conference on Robotics and Automation*, pp. 1032–1037, 1998.

[9] T. Watanabe, "Joint torque-velocity pair based manipulability for grasping system," *Proc. of IEEE/RSJ International Conference on Intelligent Robots and Systems*, pp. 2264–2270, 2008.

[10] ——, "Manipulability measures taking necessary joint torques for grasping into consideration," *Proc. 0f IEEE/RSJ International Conference on Intelligent Robots and Systems*, pp. 598–603, 10 2010.

[11] J. Kerr and B. Roth, "Analysis of multifingered hands," *The International Journal of Robotics Research*, vol. 4, no. 4, pp. 3–17, 1986.

[12] C. B. Barber, D. P. Dobkin, and H. Huhdanpaa, "The quickhull algorithm for convex hulls," *ACM Transactions on Mathematical Software*, vol. 22, no. 4, pp. 469–483, 1996.

[13] A. Miller and P. Allen, "Graspit!: A versatile simulator for grasp analysis," *ASME Int. Mechanical Engineering Congress & Exposition*, 2000.

[14] I. Kao and M. R. Cutkosky, "Quasistatic manipulation with compliance and sliding," *The International Journal of Robotics Research*, vol. 11, no. 1, pp. 20–39, 1992.

[15] N. Xydas and I. Kao, "Modeling of contact mechanics and friction limit surface for soft fingers in robotics, with experimental results," *The International Journal of Robotics Research*, vol. 18, no. 8, pp. 941–950, 1999.

[16] S. Arimoto, *Control Theory of Muli-fingered Hands*. Springer, 2008.

[17] T. Inoue and S. Hirai, "Elastic model of deformable fingertip for soft-fingered manipulation," *IEEE Transaction on Robotics*, vol. 22, no. 6, pp. 1273–2379, 2006.

[18] A. Bicchi and D. Prattichizzo, "Manipulability of cooperating robots with unactuated joints and closed-chain mechanisms," *IEEE Transactions on Robotics and Automation*, vol. 16, no. 4, pp. 336–345, 2000.

[19] J. A. Williams, "Engineering tribology," 1994.

[20] B. N. J. Persson, "Theory of rubber friction and contact mechanics," *Journal of chemical physics*, vol. 115, no. 8, pp. 3840–3861, 2001.

[21] B. N. Persson, F. Bucher, and B. Chiaia, "Elastic contact between randomly rough surfaces: Comparison of theory with numerical results," *Physical Review B*, vol. 65, no. 18, pp. 184 106:1–7, 2002.

[22] B. Persson, O. Albohr, C. Creton, and V. Peveri, "Contact area between a viscoelastic solid and a hard, randomly rough, substrate," *Journal of Chemical Physics*, vol. 120, no. 18, pp. 8779–8793, 2004.

[23] Z. Yu and Q. Wenhan, "Linearizing the soft finger contact constraint with application to dynamic force distribution in multifingered grasping," *Science in China Ser. E Engineering & Materials Science*, vol. 48, no. 2, pp. 121–130, 2005.

[24] C. Ferrari and J. Canny, "Planning optimal grasps," *Proc. of IEEE International Conference on Robotics and Automation*, pp. 2290–2295, 1992.